PHYSICAL REVIEW B **88**, 081303(R) (2013)

Long-distance radiative excitation transfer between quantum dots in disordered photonic crystal waveguides

Momchil Minkov and Vincenzo Savona
Institute of Theoretical Physics, Ecole Polytechnique Fédérale de Lausanne (EPFL), CH-1015 Lausanne, Switzerland
(Received 10 July 2013; published 19 August 2013)

We theoretically investigate the magnitude and range of the photon-mediated interaction between two quantum dots embedded in a photonic crystal waveguide, including fabrication disorder both in the crystal and in the dot positioning. We find that disorder-induced light localization has a drastic effect on the excitation transfer rate—as compared to an ideal structure—and that this rate varies widely among different disorder configurations. Nevertheless, we also find that significant rates of 50 μeV at a range of 10 μm can be achieved in realistic systems.

DOI: 10.1103/PhysRevB.88.081303 PACS number(s): 78.67.Hc, 42.50.Ct, 42.70.Qs, 03.67.−a

Semiconductor quantum dots (QDs) have very recently become candidate building blocks of a quantum-information technology, after the experimental proof of full single-qubit control.[1–8] Beyond that, the possibility for *two* qubits to interact coherently in a controlled fashion is an essential requirement for two-qubit quantum gates, which are a building block of the mainstream quantum-information protocol.[9] Given the localized nature of the quantum dots, a quantum bus is needed to provide the link between distant QD qubits.[10] In a semiconductor system, photons are an obvious choice for this task, due to their weak coupling to the environment (long decoherence time), and long-distance propagation. Additionally, semiconductor photonic crystal (PHC) devices have advanced to a remarkable level of sophistication. The state-of-the-art subnanometer fabrication precision[11–13] has brought about ultra-high-Q cavity designs[14–16] with mode volumes close to the diffraction limit, as well as low-loss, slow-light engineered waveguides.[17] This, together with the recent experimental success of Purcell-enhancing the emission of a single dot in a PHC waveguide,[18–23] and even reaching the strong coupling regime in such a structure,[24] suggests that a PHC-QD system could be an ideal candidate for demonstrating photon-mediated excitation transfer between distant dots.

Coherent interaction between two QDs at subwavelength distance in a microcavity has been recently observed.[25] At longer distance, the interaction was theoretically shown to be finite but weak (as compared to typical radiative loss and decoherence rates) in three-dimensional (bulk)[26] and two-dimensional[27] spatially homogeneous dielectric environments. The ideal compromise between interaction strength and range is thus expected in a one-dimensional environment like a PHC waveguide, and indeed, the possibility for entangled states between distant QDs coupled to such a structure has been demonstrated,[28] and the characteristic interaction distance was estimated[29] to be given by $r_{12} = 2v_g/\gamma$, where v_g is the group velocity at the exciton resonant frequency, while γ is the loss rate of the waveguide modes. However, it is known that disorder residual in the fabrication process dramatically affects the slow-light guided modes. In Ref. 29, we partially took this into account by introducing a phenomenological loss rate γ as stemming from disorder-induced (extrinsic) losses, while the assumption of a perfectly ordered PHC structure implied that the effect of Anderson localization of light[30] was not included. In this work, we simulate realistic systems with different magnitudes of the disorder, and show that while light localization indeed has a profound effect on both range and magnitude of the dot-dot excitation transfer rate, this latter is still sizable, compared to typical decoherence rates, even at several μm distance.

The waveguide studied here is formed by a missing row of holes in a triangular lattice of circular holes etched in a dielectric slab suspended in air (W1 waveguide). The specific parameters, relevant to InGaAs quantum dots in GaAs structures,[31,32] are lattice constant $a = 260$ nm, hole radius 65 nm, slab thickness 120 nm, and a real part of the refractive index $\sqrt{\varepsilon_\infty} = 3.41$. In the absence of fabrication disorder, the structure presents one-dimensional periodicity along the direction of the missing holes, thus the modes are folded into Bloch bands [Fig. 1(a)]. Everywhere below, we focus on the main guided band (blue line), in the spectral range close to the band edge [Fig. 1(b)]. Fabrication disorder is introduced in the form of random fluctuations in the x and y positions and the radius of each hole, drawn from a Gaussian random distribution with zero mean standard deviation σ. A waveguide of length $512a$ is simulated, and in the presence of disorder, its electromagnetic modes are computed by expansion on the basis of the Bloch modes of the regular structure.[30,33]

Without disorder, guided modes in the considered spectral range are lossless, as they lie below the light cone [dashed line of Fig. 1(a)] and thus do not radiate outside the slab. Disorder has several important effects. First, it mixes those modes with the ones above the light cone, introducing "extrinsic" losses, i.e. imposing a finite probability for out-of-plane radiation. Second, it limits the maximum group index, which in the ideal case goes to infinity at the band edge, and introduces modes that lie *below* the band edge of the regular structure, i.e., the density of states of the disordered guide presents a Lifshitz tail below the van Hove singularity.[30,34] In addition, disorder induces Anderson localization of light,[20,30,35] which for states close to or below the band edge can be extremely strong [Fig. 1(c)], localizing the electric field over several elementary cells. The field profiles of such modes resemble those of PHC cavities, and both strong Purcell enhancement[20] and cavity-like vacuum Rabi splitting[24] of a single QD coupled to such a mode has already been observed. Modes slightly higher in frequency become more extended, and present more than

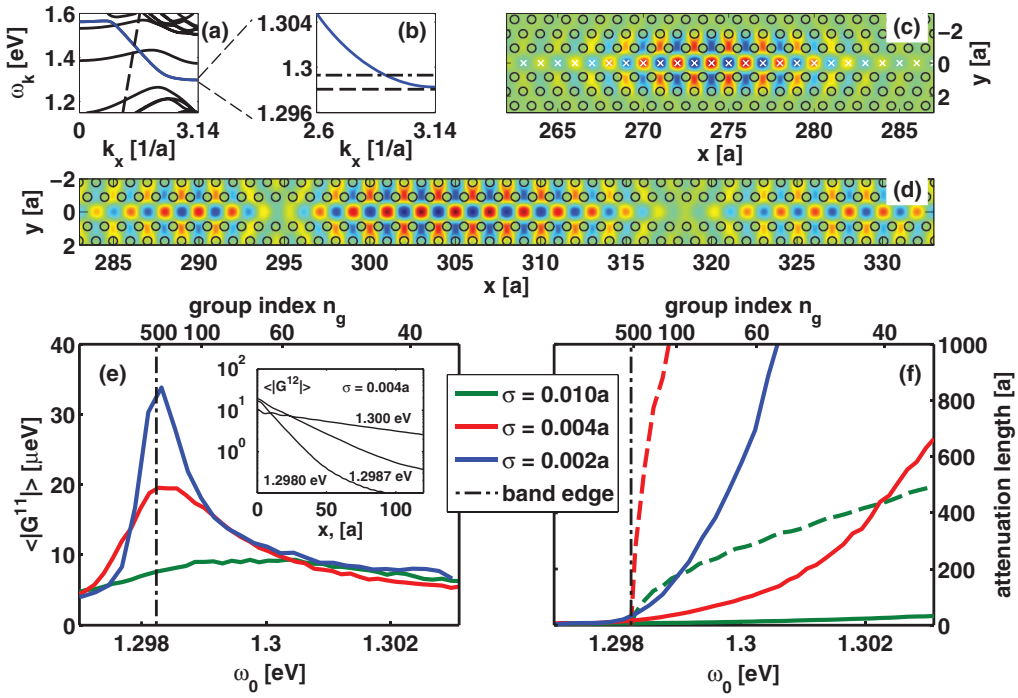

FIG. 1. (Color online) (a) Band structure of the regular waveguide; the main guided band is shown as a blue line. The dashed line represents the light cone. (b) Zoom-in close to the edge of the guided band. (c) y component of the electric field (E_y) of the mode at frequency $\omega = 1.2980$ eV [dashed line in (b)]; the white crosses indicate the elementary cell centers, where we assume a quantum dot can be placed. (d) E_y of the mode at frequency $\omega = 1.2993$ eV [dashed-dotted line in (b)]. (e) Disorder-averaged zero-distance coupling $\langle|G^{11}(\omega_0)|\rangle$, plotted as a function of the exciton frequency ω_0. (f) Characteristic decay length of the disorder-averaged coupling $\langle|G^{12}(\omega_0)|\rangle$ as a function of ω_0. Full lines: Including disorder-induced localization. Dashed lines: No localization; the decay length is simply given by $2v_g/\gamma$. In both (e) and (f), three different magnitudes of disorder have been assumed (see legend). The vertical dot-dashed line denotes the band edge of the regular waveguide. For $\sigma = 0.002a$, the $2v_g/\gamma$ curve in (f) cannot be distinguished from the band-edge line on the scale of the plot. The inset in (e) shows the disorder-averaged $\langle|G^{12}(\omega_0)|\rangle$ as a function of distance, for three different values of the exciton frequency ω_0, and $\sigma = 0.004a$.

one lobe [Fig. 1(d)], and in fact provide the ideal compromise between strength and range of the dot-dot excitation transfer. In this work, we always consider two dots in the waveguide, which are placed in the center of an elementary cell [at a position indicated by a white cross in Fig. 1(c)], and so at a distance multiple of a from each other.

To quantify the QD-W1 and the effective QD-QD coupling, we use Green's function formalism that we developed in Ref. 29 starting from Maxwell's equations for the PHC with an added linear susceptibility due to the QDs (valid in the low-excitation regime). The effective coupling strength is

$$G^{12}(\omega_0) = d^2 \frac{2\pi}{\epsilon_\infty \hbar} \frac{\omega_0^2}{c^2} G(\mathbf{r}_1, \mathbf{r}_2, \omega_0), \qquad (1)$$

where d is the dipole moment of the dot, ϵ_∞ is the dielectric constant of the semiconductor, ω_0 is the exciton resonance frequency, and $G(\mathbf{r}_1, \mathbf{r}_2, \omega_0)$ is the photonic Green's function at the dot positions, computed here using the resolvent representation once the orthonormal set of electric field modes of the waveguide is obtained through the Bloch-mode expansion. An important remark is thus that Eq. (1) takes into account the *many-mode* exciton-photon coupling that is bound to occur close to the band edge, where the density of photonic modes is high. The dipole moment d can be estimated from the spontaneous emission rate of the dot embedded in the bulk semiconductor, which was taken here to be $\Gamma = 1$ ns^{-1}. In the weak-coupling regime, the Purcell enhancement factor for a single dot in the PHC is related to the zero-distance coupling as $F_P = -2\mathrm{Im}[G^{11}(\omega_0)]/\Gamma$. More generally, $G^{11}(\omega_0) = \sum_m |g_m|^2/(\omega_m - i\gamma_m - \omega_0)$, where the sum runs over all the electromagnetic field eigenmodes, g_m is the coupling rate of the dot to each mode, while ω_m and γ_m are, respectively, the frequency and loss rate of each mode. If the coupling rate exceeds the loss rates, strong coupling is set, and in the case of both one and two dots, the irreversible radiative decay is replaced by oscillatory dynamics of the energy transfer.[29] In this sense, $G^{12}(\omega_0)$ is a measure of the frequency of this oscillatory excitation transfer process between two distant dots.

It should be noted that while localized modes always appear in the presence of disorder, their particular shape and the position of the localized lobes differ vastly among disorder realizations. Thus, here we perform the analysis using a *configuration average* over 400 different realizations of the waveguide disorder, and a *running average* over the position of the first dot in each particular waveguide. The dependence with interdot distance of the averaged magnitude of the excitation transfer rate $\langle|G^{12}|\rangle$ is shown in the inset of Fig. 1(e) for three different exciton transition frequencies ($\omega_0 = 1.2980$, $\omega_0 = 1.2987$, and $\omega_0 = 1.3000$ eV, with band edge at $\omega = 1.2982$ eV) and for $\sigma = 0.004a$. These plots show some deviation from an exponential law at large distances, but

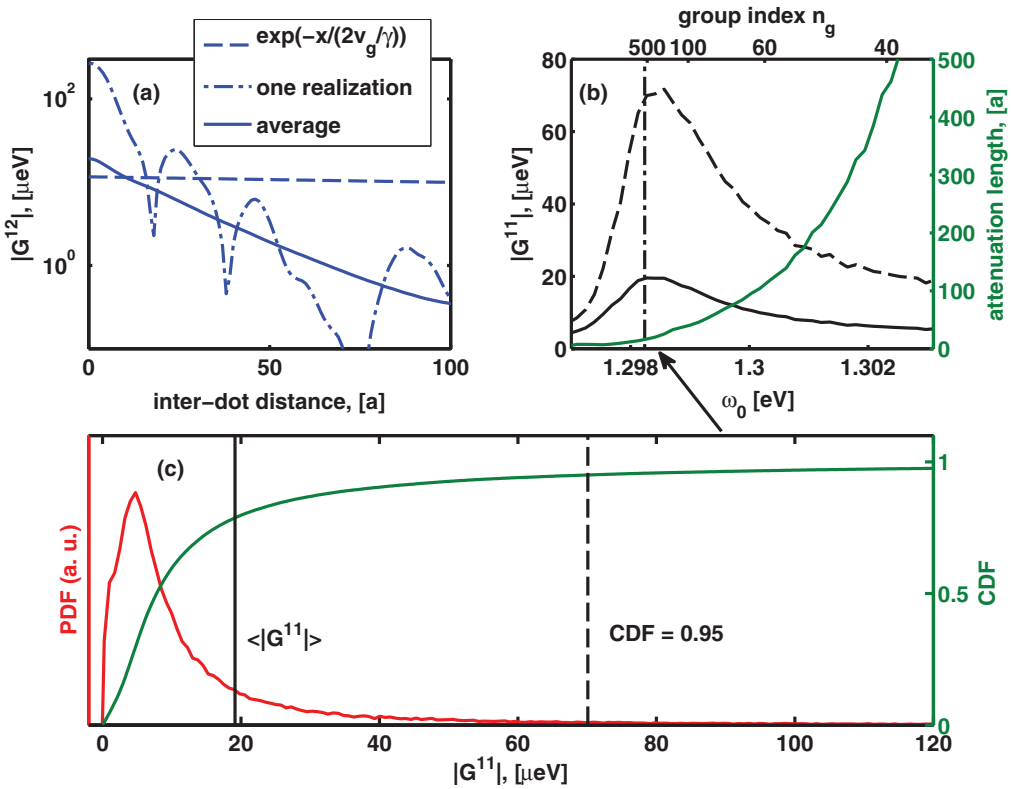

FIG. 2. (Color online) (a) Excitation transfer rate vs distance without light localization (dashed) or with for a single disorder realization (dashed-dotted) and the configuration average (solid), for $\sigma = 0.004a$ and $\omega_0 = 1.2985$ eV [indicated by an arrow in (b)]. (b) The two solid lines are the same as the $\sigma = 0.004a$ lines in Figs. 1(e) and 1(f); the dashed line shows the value of $|G^{11}|$ for which the CDF [panel (c)] is 0.95. (c): PDF and CDF of $|G^{11}|$, with $\langle|G^{11}|\rangle$ and the CDF = 0.95 values explicitly indicated.

this is an unphysical result originating form the finite size of our simulation domain, and occurs at very small values of G^{12} which are scarcely relevant to our conclusions. For each ω_0, an exponential function can thus be fitted in the region where the decay is a straight line on a logarithmic plot, and an attenuation length can be extracted. On this basis, Figs. 1(e) and 1(f) give detailed information about the dot-dot interaction for three different disorder magnitudes. The strength is quantified in Fig. 1(e), through the averaged zero-distance term $\langle|G^{12}|\rangle$, while the range—in Fig. 1(f) through the interpolated attenuation length. Finally, even though the group index n_g cannot be well-defined in the presence of localization, its value in the ideal-PHC case is given on the top x axis in both figures.

Some previous experimental works[20,24] in which single-dot coupling to a PHC waveguide has been demonstrated take advantage of large PHC disorder as a means to have strongly localized modes. That this is beneficial is not directly obvious from the large-disorder result shown in Fig. 1(e), which never exceeds 10 μeV. It should be kept in mind, however, that this result represents the configuration-averaged zero-distance coupling. In a few individual configurations in which the dot is sitting exactly on top of a strongly localized mode, the same coupling can exceed 100 μeV. In any case, such a strong disorder makes it very unlikely to have long-distance dot-dot interaction, as can be seen from Fig. 1(f). For $\sigma = 0.004a$ ($\approx$1 nm in typical systems, realistically achievable), however, the attenuation length becomes sizable—on the order of $100a$ which corresponds to the 10 μm range. Notice, though, that the localization still has a drastic effect as compared to the case of extrinsic losses only, where the transfer rate is determined by the ratio $2v_g/\gamma$ plotted as dashed lines in Fig. 1(f), which was analyzed in Ref. [29]. In the figure, γ was taken as the average over the loss rates, computed through Bloch-mode expansion, for each of the disorder magnitudes, and corresponds to a quality factor of $\mathcal{Q} = 95\,000$ for each mode in the $\sigma = 0.004a$ case. The drastic influence of Anderson localization emerges in the fact that modes at a given frequency are characterized by a localization length which also determines the spatial decay of the light transport process at that frequency. The corresponding decay length is generally much smaller than that associated with *ballistic* propagation in the presence of a phenomenological extrinsic loss rate, as studied in Ref. 29. In the context of light propagation in PHCs, the effect of Anderson localization is often referred to as *backscattering losses*,[36–38] and was shown to severely degrade the transmission for frequencies close to the band edge.

While the configuration average gives a good estimate of the interaction strength, it is also important to understand the underlying statistics, to know what one could expect in an actual experiment. In Fig. 2(a), we plot the coupling $|G^{12}(\omega_0)|$ as a function of the dot-dot distance for $\sigma = 0.004a$ and $\omega_0 = 1.2985$ eV [indicated by an arrow in Fig. 2(b)]. The full line is the configuration-averaged quantity, the dashed line represents the $\exp[-x/(2v_g/\gamma)]$ dependence (namely,

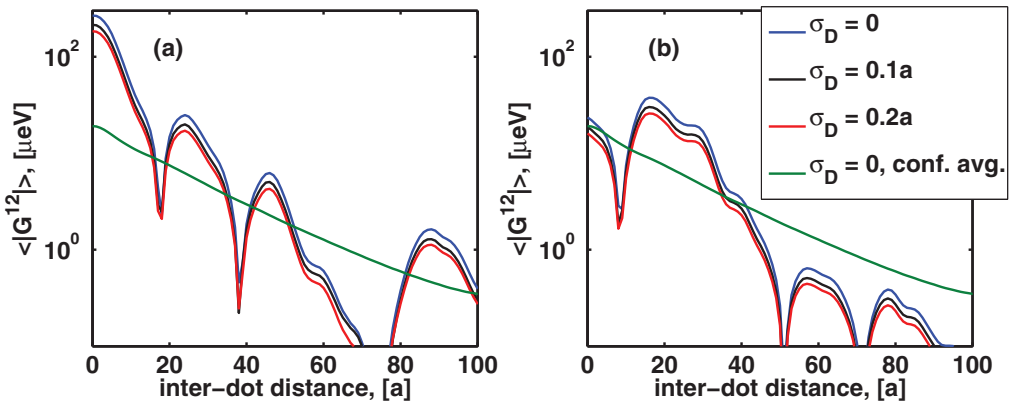

FIG. 3. (Color online) For two different positions of the first dot, the excitation transfer rate as a function of dot-dot distance, for the dots placed exactly at the center of the elementary cells (blue line) and with some positioning disorder corresponding to a finite value of σ_D (black and red lines, averaged over dot positioning). The configuration average over PHC disorder is also shown (green line).

neglecting localization effects), while the dot-dashed line represents a single disorder realization. As a first remark, when neglecting localization effects the coupling decays very slowly, illustrating again the difference that localization effects make. When accounting for localization instead, the coupling decays significantly with distance, but its magnitude at short distances is increased. This enhancement is due to the presence of modes localized on a short spatial range, which behave similarly to resonant cavity modes. The disorder configuration and the position of the first dot were selected from the statistical ensemble in order to have a large zero-distance coupling, exceeding 100 μeV. This is suggestive of the fact that the statistics are characterized by a large variance. As a better illustration, we compute the statistical distribution of the values of $|G^{11}|$ [for the same parameters as in Fig. 2(a)] and plot it in Fig. 2(c). The distribution exhibits a very long tail towards high values, suggesting that there is a sizable probability of having large radiative coupling. This is highlighted in Fig. 2(b) where we plot, as a function of ω_0, the configuration-averaged value of $|G^{11}|$ (full line) and compare it to the value for which the cumulative distribution function (CDF) is equal to 0.95 (dashed line). Put simply, the dashed line in Fig. 2(b) gives the magnitude of the coupling that one can expect from 1 in every 20 samples. It is then clear that $|G^{11}|$ can exceed 70 μeV, and a value of above 30 μeV can be expected even for frequencies for which the interaction range is of the order of $100a$.

It is important to note that the PHC disorder plays a more important—and nontrivial—role than the imperfect positioning of the quantum dots. To illustrate this fact, we take one specific disorder realization of the PHC waveguide, place one QD at the center of an elementary cell of the waveguide, while for the second QD—located in another elementary cell of the guide—we assume a random displacement from the center of the cell, characterized by a Gauss distribution with standard deviation σ_D. Figures 3(a) and 3(b) show the computed dot-dot coupling $|G^{12}(\omega_0)|$ for a selected realization of the PHC disorder and with the first dot placed in two different elementary cells, as a function of the interdot distance expressed as an integer multiple of the lattice parameter a. Parameters are $\sigma = 0.004a$ and $\omega_0 = 1.2985$ eV. In both panels, the green line denotes the corresponding quantity averaged over the disorder realizations, while the other curves are computed for a single realization and different values of σ_D, and are averaged over the position of the second QD. The only effect of a finite value of σ_D is a rescaling of the interdot coupling by a factor not far from unity, which is expected, because the electric field does not vary strongly on the length scale of a few tens of nanometers.

In conclusion, in this work we investigated the possibility for excitation transfer between distant quantum dots in a photonic crystal waveguide. Due to Anderson localization of light, disorder in the position and size of the PHC holes was found to have a highly nontrivial effect on the interaction, thus statistics based on 400 different disorder realizations were analyzed. For $\sigma = 0.004a$, the averaged excitation transfer rate was found to be larger than 10 μeV at distances on the order of 10 μm. In addition, in a 1-out-of-20 setting, the rate reaches 50 μeV and more. The transfer time to which this corresponds is on the order of 10 ps—close to the single-qubit operation time and much shorter than the decoherence time measured in these systems. Disorder in the positioning of the dots has a straightforward scaling down effect, which is small when the precision is in the range of tens of nanometers. This shows that a PHC waveguide or a similar structure engineered to further enhance the dot-dot coupling is an ideal candidate for establishing a long-distance, photon-mediated QD state transfer.

This work was supported by the Swiss National Science Foundation through Project No. 200020_132407.

[1] B. Patton, U. Woggon, and W. Langbein, Phys. Rev. Lett. **95**, 266401 (2005).

[2] D. Press, T. D. Ladd, B. Zhang, and Y. Yamamoto, Nature **456**, 218 (2008).

[3] J. Berezovsky, M. H. Mikkelsen, N. G. Stoltz, L. A. Coldren, and D. D. Awschalom, Science **320**, 349 (2008).

[4] A. Greilich, S. E. Economou, S. Spatzek, D. R. Yakovlev, D. Reuter, A. D. Wieck, T. L. Reinecke, and M. Bayer, Nat. Phys. **5**, 262 (2009).

[5] A. Greilich, S. G. Carter, D. Kim, A. S. Bracker, and D. Gammon, Nat. Photon. **5**, 703 (2011).
[6] E. Poem, O. Kenneth, Y. Kodriano, Y. Benny, S. Khatsevich, J. E. Avron, and D. Gershoni, Phys. Rev. Lett. **107**, 087401 (2011).
[7] K. Müller, A. Bechtold, C. Ruppert, C. Hautmann, J. S. Wildmann, T. Kaldewey, M. Bichler, H. J. Krenner, G. Abstreiter, M. Betz, and J. J. Finley, Phys. Rev. B **85**, 241306 (2012).
[8] T. M. Godden, J. H. Quilter, A. J. Ramsay, Y. Wu, P. Brereton, S. J. Boyle, I. J. Luxmoore, J. Puebla-Nunez, A. M. Fox, and M. S. Skolnick, Phys. Rev. Lett. **108**, 017402 (2012).
[9] M. A. Nielsen and I. L. Chuang, *Quantum Computation and Quantum Information*, Cambridge Series on Information and the Natural Sciences, 1st ed. (Cambridge University, New York, 2004).
[10] H. J. Kimble, Nature **453**, 1023 (2008).
[11] S. L. Portalupi, M. Galli, M. Belotti, L. C. Andreani, T. F. Krauss, and L. O'Faolain, Phys. Rev. B **84**, 045423 (2011).
[12] Y. Taguchi, Y. Takahashi, Y. Sato, T. Asano, and S. Noda, Opt. Express **19**, 11916 (2011).
[13] N. L. Thomas, Z. Diao, H. Zhang, and R. Houdre, J. Vac. Sci. Technol. B **29**, 051601 (2011).
[14] Y. Akahane, T. Asano, B. Song, and S. Noda, Nature **425**, 944 (2003).
[15] B. Song, S. Noda, T. Asano, and Y. Akahane, Nat. Mater. **4**, 207 (2005).
[16] E. Kuramochi, M. Notomi, S. Mitsugi, A. Shinya, T. Tanabe, and T. Watanabe, Appl. Phys. Lett. **88**, 041112 (2006).
[17] T. Baba, Nat. Photon. **2**, 465 (2008).
[18] E. Viasnoff-Schwoob, C. Weisbuch, H. Benisty, S. Olivier, S. Varoutsis, I. Robert-Philip, R. Houdré, and C. J. M. Smith, Phys. Rev. Lett. **95**, 183901 (2005).
[19] T. Lund-Hansen, S. Stobbe, B. Julsgaard, H. Thyrrestrup, T. Sünner, M. Kamp, A. Forchel, and P. Lodahl, Phys. Rev. Lett. **101**, 113903 (2008).
[20] L. Sapienza, H. Thyrrestrup, S. Stobbe, P. D. Garcia, S. Smolka, and P. Lodahl, Science **327**, 1352 (2010).
[21] A. Schwagmann, S. Kalliakos, I. Farrer, J. P. Griffiths, G. A. C. Jones, D. A. Ritchie, and A. J. Shields, Appl. Phys. Lett. **99**, 261108 (2011).
[22] T. B. Hoang, J. Beetz, L. Midolo, M. Skacel, M. Lermer, M. Kamp, S. Hofling, L. Balet, N. Chauvin, and A. Fiore, Appl. Phys. Lett. **100**, 061122 (2012).
[23] A. Laucht, T. Gunthner, S. Putz, R. Saive, S. Frederick, N. Hauke, M. Bichler, M.-C. Amann, A. W. Holleitner, M. Kaniber, and J. J. Finley, J. Appl. Phys. **112**, 093520 (2012).
[24] J. Gao, S. Combrie, B. Liang, P. Schmitteckert, G. Lehoucq, S. Xavier, X. Xu, K. Busch, D. L. Huffaker, A. De Rossi, and C. W. Wong, Scientific Reports **3**, 1994 (2013).
[25] F. Albert, K. Sivalertporn, J. Kasprzak, M. Strau, C. Schneider, S. Hfling, M. Kamp, A. Forchel, S. Reitzenstein, E. A. Muljarov, and W. Langbein, Nat. Commun. **4**, 1747 (2013).
[26] G. Parascandolo and V. Savona, Phys. Rev. B **71**, 045335 (2005).
[27] G. Tarel, G. Parascandolo, and V. Savona, Phys. Status Solidi B **245**, 1085 (2008).
[28] P. Yao and S. Hughes, Opt. Express **17**, 11505 (2009).
[29] M. Minkov and V. Savona, Phys. Rev. B **87**, 125306 (2013).
[30] V. Savona, Phys. Rev. B **83**, 085301 (2011).
[31] A. Faraon, I. Fushman, D. Englund, N. Stoltz, P. Petroff, and J. Vuckovic, Nat. Phys. **4**, 859 (2008).
[32] A. Reinhard, T. Volz, M. Winger, A. Badolato, K. J. Hennessy, E. L. Hu, and A. Imamoglu, Nat. Photon. **6**, 93 (2012).
[33] V. Savona, Phys. Rev. B **86**, 079907(E) (2012).
[34] S. R. Huisman, G. Ctistis, S. Stobbe, A. P. Mosk, J. L. Herek, A. Lagendijk, P. Lodahl, W. L. Vos, and P. W. H. Pinkse, Phys. Rev. B **86**, 155154 (2012).
[35] J. Topolancik, B. Ilic, and F. Vollmer, Phys. Rev. Lett. **99**, 253901 (2007).
[36] S. Hughes, L. Ramunno, J. F. Young, and J. E. Sipe, Phys. Rev. Lett. **94**, 033903 (2005).
[37] L. O'Faolain, T. P. White, D. O'Brien, X. Yuan, M. D. Settle, and T. F. Krauss, Opt. Express **15**, 13129 (2007).
[38] S. Mazoyer, P. Lalanne, J. Rodier, J. Hugonin, M. Spasenović, L. Kuipers, D. Beggs, and T. Krauss, Opt. Express **18**, 14654 (2010).